Undulations in Subducted Oceanic Crust Correlate With Shallow Tremor Distribution in the Kuril Trench Off Hokkaido

Yamaguchi, Hiroto ; Kodaira, Shuichi ; Fujie, Gou ; No, Tetsuo ; Nakamura, Yasuyuki ; Shiraishi, Kazuya ; Seama, Nobukazu

(Citation)
Geophysical Research Letters,51(1):e2023GL106815

(Issue Date)
2024-01-16

(Resource Type)
journal article

(Version)
Version of Record

(URL)
https://hdl.handle.net/20.500.14094/0100486289

Geophysical Research Letters

RESEARCH LETTER
10.1029/2023GL106815

Key Points:

- Seismic reflection surveys in the Kuril Trench image undulations in the subducted oceanic crust, as well as strong overlying reflectors
- Amplitudes and wavelengths of undulations correlate with shallow tremor occurrences
- Undulations and the distribution of strong reflections on the plate boundaries shown in previous studies also generally correspond

Supporting Information:

Supporting Information may be found in the online version of this article.

Correspondence to:

H. Yamaguchi,
hiroyama3val.ma2@stu.kobe-u.ac.jp

Citation:

Yamaguchi, H., Kodaira, S., Fujie, G., No, T., Nakamura, Y., Shiraishi, K., & Seama, N. (2024). Undulations in subducted oceanic crust correlate with shallow tremor distribution in the Kuril Trench off Hokkaido. *Geophysical Research Letters*, *51*, e2023GL106815. https://doi.org/10.1029/2023GL106815

Received 17 OCT 2023
Accepted 19 DEC 2023

Undulations in Subducted Oceanic Crust Correlate With Shallow Tremor Distribution in the Kuril Trench Off Hokkaido

Hiroto Yamaguchi[1,2], Shuichi Kodaira[2,3], Gou Fujie[2], Tetsuo No[2], Yasuyuki Nakamura[2], Kazuya Shiraishi[2], and Nobukazu Seama[1,3]

[1]Department of Planetology, Graduate School of Science, Kobe University, Kobe, Japan, [2]Research Institute for Marine Geodynamics, Japan Agency for Marine-Earth Science and Technology, Yokohama, Japan, [3]Kobe Ocean-Bottom Exploration Center, Kobe University, Kobe, Japan

Abstract Recent research has shown that shallow tremors tend to occur in spatial association with heterogeneous conditions, which are formed by seamounts or ridges on the subducted oceanic crust. In the southern Kuril Trench, shallow tremors have been observed on the western side, although no apparent heterogeneity in the subducted oceanic crust has been identified. To investigate structures spatially associated with these shallow tremors, we processed reflection seismic data acquired along seven profiles. We examined structures ranging from the seafloor to the top of the oceanic crust, within a depth of up to 20 km. Our results reveal that undulations observed at the top of the subducted oceanic crust are related to the distribution and number of shallow tremors. The undulations would play a crucial role in the distribution of shallow tremors.

Plain Language Summary Shallow tremors, often occurring near subducted seamounts and ridges underground, are small earthquakes that take place at shallower depths of a plate boundary compared to megathrust earthquakes. While the mechanisms behind these two types of earthquakes are not yet fully comprehended, there is an observed correlation, particularly in terms of their locations. At the southern Kuril Trench, shallow tremors have only been detected on the western side, where there aren't any subducted seamounts or ridges. Seismic surveys carried out in the southern Kuril Trench have provided detailed images of the subsurface structures. These images indicate that shallow tremors are more likely to happen in areas where the subducted oceanic crust has pronounced undulations. It's worth noting that only these undulations on the oceanic crust—and not other significant structures—have been linked to the occurrence of shallow tremors.

1. Introduction

Shallow tremors occur along the plate interface, but at shallower depths than the seismogenic zone of megathrust earthquakes (Obara & Kato, 2016), and they have been widely observed in subduction zones in Costa Rica (Walter et al., 2011), New Zealand (Todd et al., 2018), northeast Japan (Nishikawa et al., 2019), and the Nankai Trough (Obana & Kodaira, 2009). The locations of shallow tremors provide essential information about the frictional properties and, thus, the mechanical behavior of the plate interface (Walter et al., 2011). Shallow tremor distributions are strongly linked to structural heterogeneities such as seamounts and ridges (Yokota et al., 2016). For example, at the North Hikurangi subduction zone in New Zealand, shallow tremors occur in relation to a seamount 40 km long, 15 km wide, and with a relative elevation of 2.5 km (Barker et al., 2018; Todd et al., 2018). In the Nankai Trough at Hyuga-nada, a subduction ridge more than 50 km wide and with a relative elevation of 1.5 km (Park et al., 2009) is considered to contribute to the occurrence of shallow tremors (Yamashita et al., 2015, 2021). Indeed, numerical modeling indicates that a subducting seamount significantly alters the surrounding slip behavior (Sun et al., 2020).

Shallow tremors detected along the Japan Trench have also been attributed to various physical characteristics of the plate-boundary materials (Nishikawa et al., 2023). The Seafloor Observation Network for Earthquakes and Tsunamis along the Japan Trench (S-net) has revealed the detailed distribution of shallow tremors along both the Japan and Kuril Trenches (NIED, 2019). Specifically, shallow tremors at Ibaraki-oki occur in a section of the subducted oceanic crust characterized by low *P*-wave velocities (Hua et al., 2020), which are attributed to the presence of fluids or hydrous minerals at the plate boundary (Mochizuki et al., 2005; Nishikawa et al., 2023). Shallow tremors in the Iwate-oki region are closely associated with an area suggested to be undergoing sediment

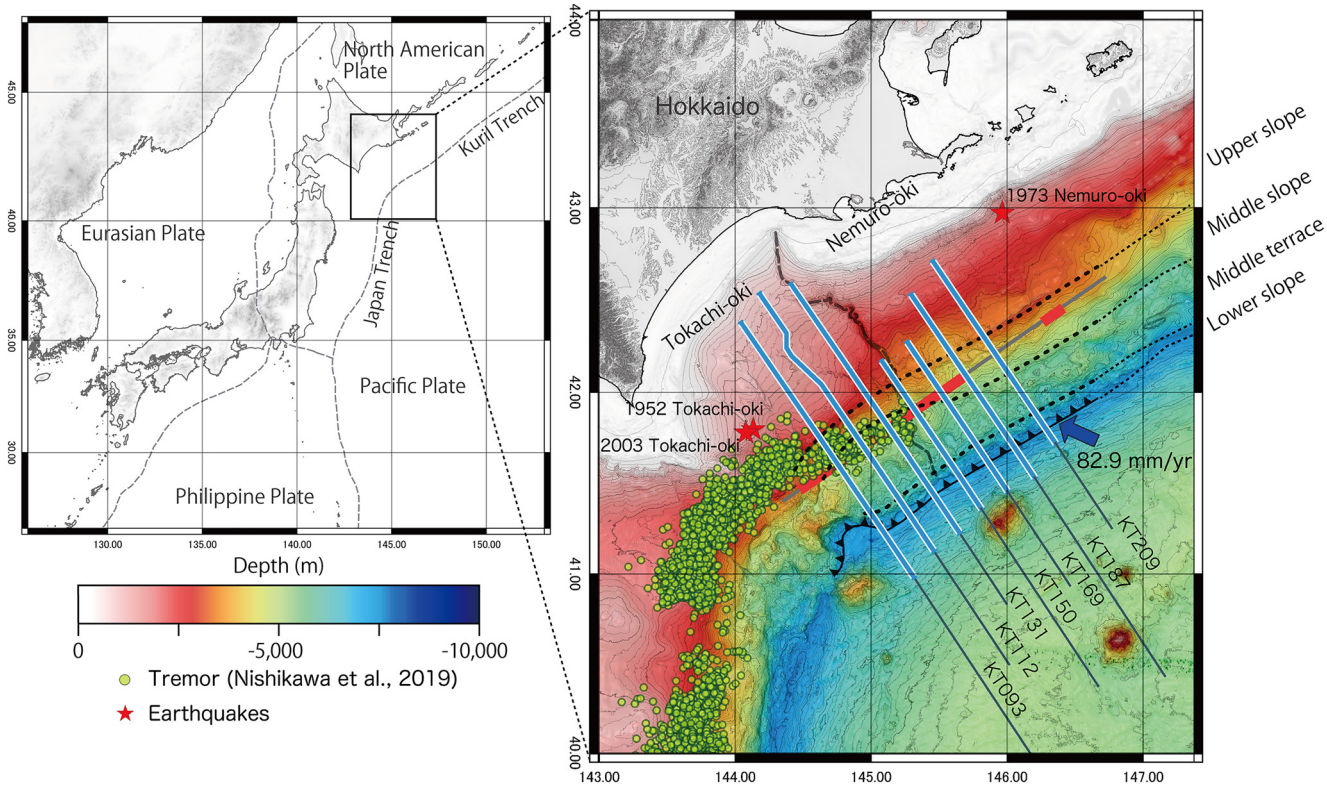

Figure 1. Maps indicating the study area and the seismic profiles used herein (thin blue lines). Portions of the seismic profiles outlined in white indicate the areas shown in Figures 2 and 3a. Green dots indicate shallow tremor events determined by Nishikawa et al. (2019). The three dashed and dotted lines parallel to the trench, as well as the trace of the trench itself, delimit the topographic divisions of Okamura et al. (2008). The heavy dashed line roughly perpendicular to the trench is the Kushiro Submarine Canyon. Red stars indicate the epicenters of three major earthquakes from Japan Meteorological Agency hypocenter data. The bold gray line is the survey line of Azuma et al. (2012); portions highlighted by thick red lines are the strong plate boundary reflections they reported. The topography is used GEBCO 2022 Grid (GEBCO Compilation Group, 2022).

metamorphism (Fujie et al., 2020). There, petit-spot volcanism has disrupted the pre-existing stratigraphy and transformed pelagic sediments into patchy distribution of minerals with high coefficients of friction (Fujie et al., 2020). Nishikawa et al. (2023) suggested that the occurrence of shallow tremors at the plate boundary may result from the subduction of materials with varied coefficients of friction.

In the Kuril Trench off Hokkaido, shallow tremors along the plate boundary have been observed only on the western side of the trench (Nishikawa et al., 2019). The tremor distribution is obtained from data acquired by S-net in 2016–2018, but it should be noted that a similar shallow tremor distribution was observed in the same region in 2006–2007 (Kawakubo et al., 2020) even before the 2011 Tohoku-oki earthquake. Previous seismic reflection surveys have imaged the subducted oceanic crust within 30 km of the trench (Okamura et al., 2008; Schnürle et al., 1995), but no structural variations such as seamounts have been identified along the plate interface in this area. Refraction seismic surveys along several survey lines have revealed laterally uniform *P*-wave velocities within the overriding plate in the trench-parallel direction (Azuma et al., 2012), and no structural anomalies such as seamounts have been observed in the subducted oceanic crust in the trench-vertical direction (Nakanishi et al., 2009). However, no seismic reflection surveys have covered the area 30–70 km landward from the trench, that is, where shallow tremors are observed off Hokkaido. Therefore, the detailed velocity and crustal structures in those areas, which are likely linked to the shallow tremors, have yet to be determined.

In this investigation, we utilized multichannel seismic (MCS) reflection survey profiles along the Kuril Trench off Hokkaido (Figure 1) to analyze the crustal structure from the seafloor to the subducted oceanic crust and to identify structures that correlate with shallow tremor occurrences. We quantified and correlated several distinct structures to better understand shallow tremor activity. Based on these findings, we discuss structures related to the occurrence of shallow tremors.

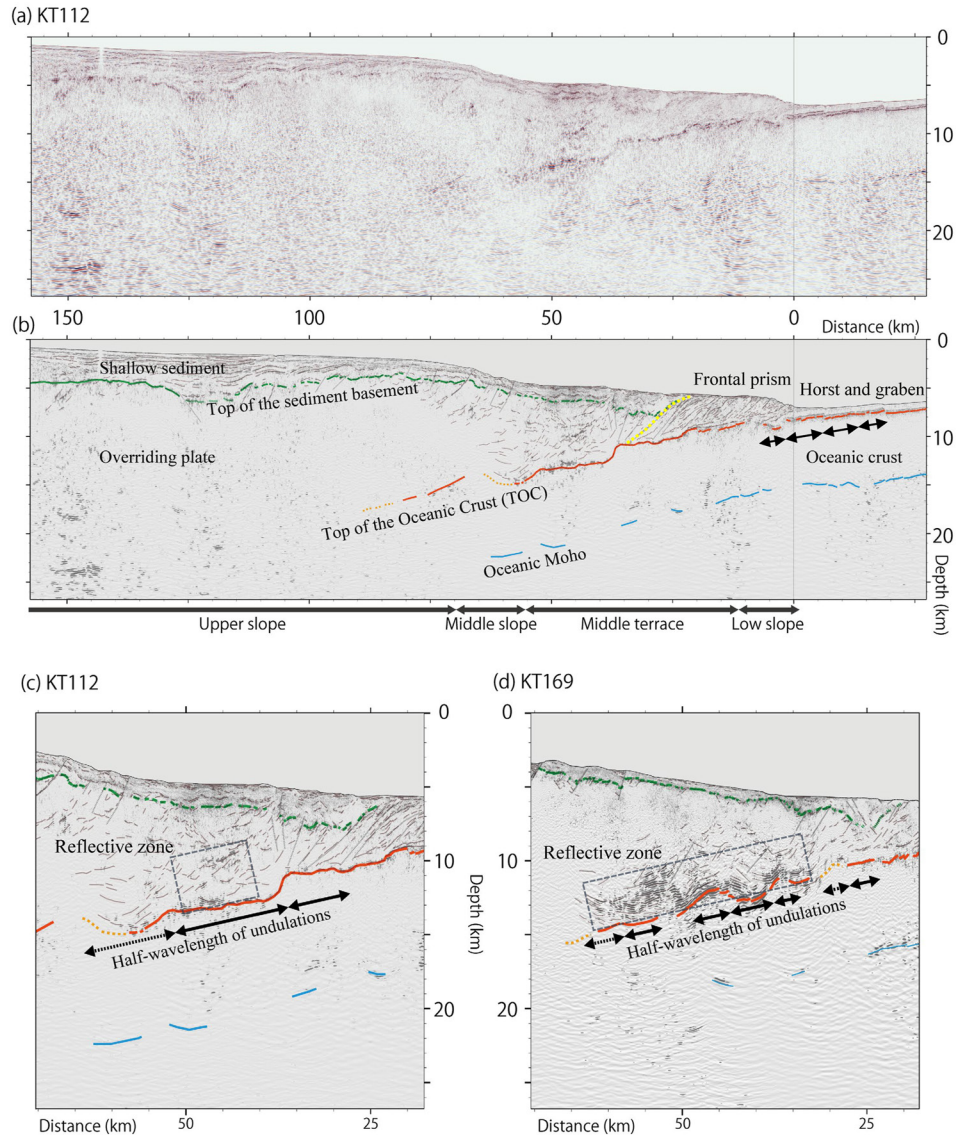

Figure 2. (a) Raw and (b–d) interpreted pre-stack depth migration sections along profiles (a–c) KT112 and (d) KT169. Green lines indicate the top of the sediment basement. Solid orange lines show the top of the oceanic crust when it is continuous and clear, whereas dotted orange lines are the interpreted top of the oceanic crust when it is more ambiguous. Blue lines denote the oceanic Moho. Dotted yellow lines are the interpreted frontal prism contacted plane. (c) In the west of the study area, the half-wavelengths of undulations in the top of the oceanic crust are over 10 km. In contrast, (d) in the east of the study area, the half-wavelengths of undulations in the top of the oceanic crust are ~5 km. Vertical exaggeration is 2:1.

2. Tectonic and Geological Background

The Kuril Trench is the boundary between the Pacific and North American Plates. The Pacific Plate converges in a west-northwest direction (294° in the study area) at a rate of 80–90 mm per year (specifically 82.9 mm per year in the study area), considering the North American Plate as fixed (calculated from NNR-MORVEL56 plate velocities; Argus et al., 2011). Numerous large earthquakes have occurred off Hokkaido. Magnitude 8-class large earthquakes there include the 1952 Tokachi-oki earthquake (Mw8.1; Hirata et al., 2003), the 1973 Nemuro-oki earthquake (Mw8,0; Nishimura, 2009), and the 2003 Tokachi-oki earthquake (Mw8.0) (Tanioka et al., 2004; Yamanaka & Kikuchi, 2003) (see Figure 1). Where the western end of the Kuril Trench intersects the Japan Trench, a subducting seamount has been observed at a shallow depth (Tsuru et al., 2005). The Kushiro submarine canyon is in the center of our research area; this vast canyon extends approximately 150 km from the shore to the trench (Okamura et al., 2008; Tuzino & Noda, 2010).

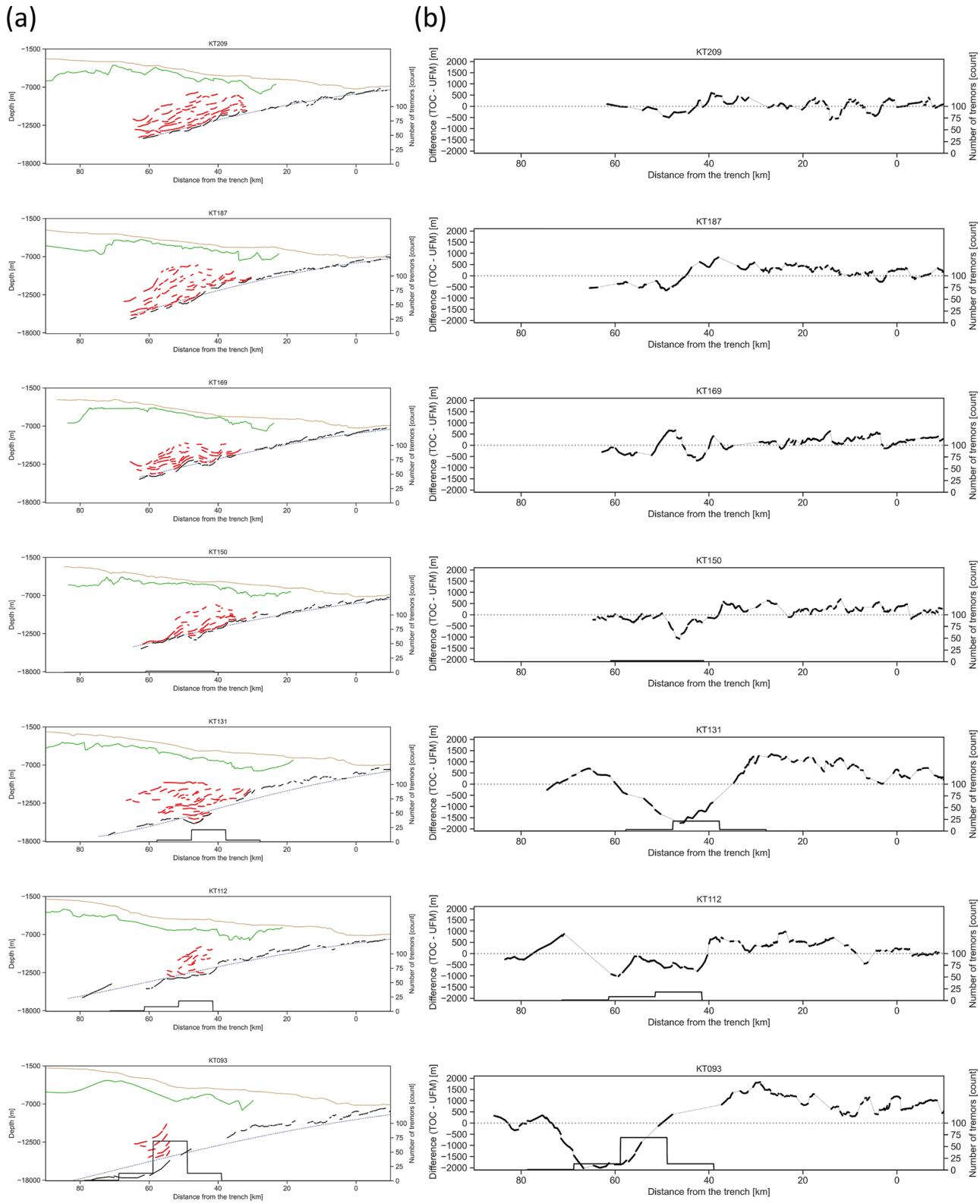

Figure 3. (a) Profiles showing the seafloor topography (brown lines) and, from seismic reflection sections, interpretations of the top of the sediment basement (green lines), strong reflections in the reflective zone (red lines), and the top of the oceanic crust (black lines). The dashed purple lines show the expected top of the oceanic crust based on the Universal Flexure Model (UFM). Bar charts (right *y*-axis) indicate the number of shallow tremors recorded in 10-km bins (see Figure 1 and Figure S1 in Supporting Information S1). (b) The difference between the expected depth to the top of the oceanic crust (from the UFM) and that observed in the reflection profiles; bar charts are as in panel (a). Vertical exaggeration is (a) 2:1 and (b) 5:1.

We divided the slope on the overriding plate (i.e., landward of the trench) into four distinct areas based on the landform categorization of Okamura et al. (2008): from shallowest to deepest, these are the "upper slope," "middle slope," "middle terrace," and "lower slope" (Figure 1). The upper slope includes areas shallower than the topographic ridge at approximately 3,200 m depth, which defines the boundary between the upper and middle slopes. The middle slope is the area between the topographic ridge and the middle terrace, which is a narrow, relatively flat area at depths of around 5,200 m in the east of the study area and approximately 5,000 m on the western side of Kushiro canyon. Finally, the lower slope includes areas downslope of the middle terrace, extending to the bottom of the trench.

3. Data and Method

The MCS reflection data is acquired along seven transects in 2019–2021 aboard the Japan Agency for Marine-Earth Science and Technology (JAMSTEC) R/Vs *Kairei* and *Kaimei*. The transects extended from the frontal prism on the Pacific Plate to the slope of the continental shelf across the western Kuril trench (Figure 1). The lines crossing the Kuril trench are within 70 km of Kushiro canyon. Along profiles KT209, KT187, KT169, and KT150, the seismic source was the *Kairei*'s tuned air gun array, which has a maximum volume of 7,800 cubic inches; the shooting interval was 50 m (KT187, KT169, KT150) or 200 m (KT209). Along profiles KT131, KT112, and KT093, the seismic source was *Kaimei*'s tuned air gun array, which has a maximum volume of 10,600 cubic inches; the shooting interval was 50 m for these four transects. To record seismic waves from the air gun shots, a common hydrophone streamer cable 5.5 km long with 444 receiver channels spaced at 12.5 m intervals was towed at 10 m depth below the sea surface. The positions of the sources and receivers were determined using the Global Navigation Satellite System. The receiver sampling rate was 2 ms. Reflection data were processed by pre-stack depth migration using grid tomography after noise reduction and signal enhancement processes by JGI, Inc. (Tokyo, Japan) to produce seismic depth profiles.

The distribution of shallow tremors was analyzed from the shallow tremor data (August 2016 to August 2018) of Nishikawa et al. (2019) using quadrat analysis, a type of point pattern analysis. We divided the study area into equal-sized 10 km × 10 km subsections, counted the number of points within each subsection, and calculated the point frequency. The sides of the subsections were oriented parallel to the survey lines, which strike of 34.1°W. A histogram representing the distribution of shallow tremors was then generated by binning the along-profile distances from the trench into the subsections intersect each survey line (see Figure 3). The total number of tremors along each survey line was calculated as the sum of the number of shallow tremors in all subsections intersecting the survey line.

4. Results

The reflection sections clearly resolved the shallow part of the overriding plate down to the uppermost mantle of the subducted oceanic crust. Structural variations at the plate boundary, such as undulations and strongly reflective zones, were resolved to 14–20 km depth over 60 km landward from the trench. In this section, we comprehensively describe the structures observed in both the shallow and deep parts of the sections.

4.1. Shallow Parts: Sediment, Basement and Frontal Prism

The shallow sediment structures of the overriding plate exhibit excellent lateral continuity, whereas faulting structures displacing the basement vary from east to west (Figure 3a). Along the upper slope, strata fill the underlying basin structures. The basement dips landward along the three westernmost survey lines (KT093, KT112, KT131), but dips trenchward along the easternmost survey lines (KT187, KT209) (green lines in Figure 3a). A normal fault is observed beneath the topographic ridge separating the upper and middle slopes along the easternmost survey lines KT169, KT187, and KT209. Displacement on this fault exceeds 1,000 m, but no such fault is visible along the survey lines to the west of KT131 (for details, see Figure S2–S4 in Supporting Information S1). Along the middle and lower slopes, sediment reflections show contorted or chaotic patterns. Sediment thicknesses are 300–800 m thicker along the western survey lines (KT093, KT112, KT131, KT150) than along the eastern lines.

A prism-shaped structure dominated by seaward-thrusting reflections is present at the toe of the overriding plate. We refer to this structure as the frontal prism, following previous studies (von Huene et al., 2009) (see Figure 2b). The frontal prism has been identified from the central Japan Trench to the central Kuril Trench (Klaeschen et al., 1994; Kodaira et al., 2017; Schnürle et al., 1995). We used the lengths of the top and bottom surfaces as well

as the prism thickness to characterize the shape of the frontal prism, following Kodaira et al. (2017; see Figure S7 in Supporting Information S1).

4.2. Deep Parts: Subducted Oceanic Crust and the Reflective Zone

The subducted oceanic crust was imaged continuously up to 80 km landward from the trench (see Figure 2b), and for an additional 10–18 km in profiles KT131, KT112, and KT093 (Figure 3, Figure S2–S4 in Supporting Information S1). Undulations of the oceanic basement, that is, at top of the oceanic crust, were identified with amplitudes exceeding 1 km and half-wavelengths of 5–40 km. Amplitudes and half-wavelengths varied among the survey lines. The most pronounced differences were observed at depths ≥12 km. Specifically, undulations in the westernmost lines (KT093, KT112, KT131) showed more significant deformation, with larger amplitudes (>1,500 m) and longer half-wavelengths (10–20 km) than those (<1,000 m and ≤5 km, respectively) in the eastern lines (KT150, KT169, KT187, KT209). Qualitatively, therefore, the top of the subducted oceanic crust shows intense undulations in the west and gentler undulations in the east. We will quantitatively evaluate these undulations in Section 5. At shallower depths, however, undulations along all survey lines showed similar half-wavelengths of about 5 km and smaller amplitudes (see Figure 3). This half-wavelength matches the width of the horst-and-graben structure formed in the oceanic crust prior to subduction (Figures 2 and 3a).

Clusters of scattered strong reflections, each less than 5 km long, were observed above the oceanic crust in each profile (Figures 2d and 3a). Here, we refer to these clusters as "the reflective zone." This zone is observed at 30–70 km landward of the trench and at depths of 7–15 km. The reflections within the reflective zone are subparallel to the subducted oceanic crust. In the east, the reflective zone extends over a length of 30 km, whereas it is significantly shorter in the west (only 3 and 13 km long along profiles KT093 and KT112, respectively). The lengths, thicknesses, and locations of the reflective zone in each profile are reported in Table S1 in Supporting Information S1. We are unaware of any report of similar structures in the Kuril Trench.

5. Discussion

Our mapping of the shallow and deep structures allowed us to quantify their respective lengths, locations, and thicknesses (see Table S1 in Supporting Information S1), which vary depending on the structure. However, no structure type other than undulations exclusively correlated with shallow tremor occurrence or could satisfactorily explain the tremor distribution (see Figure S5 in Supporting Information S1).

Comparison of the shallow tremor distribution and the structures identified in this study reveals a notable pattern: shallow tremors tend to occur in near areas characterized by intense undulations in the oceanic crust, rather than near regions with gentler undulations (see Figure 3). To further investigate the relationship between shallow tremor activity and these structural undulations, we quantified the scale of the undulations by fitting the top of the oceanic crust to the Universal Flexure Model (UFM; Turcotte & Schubert, 2001) and calculating the root-mean-square (RMS) difference between the modeled and observed depths to the top of the oceanic crust. The UFM is a mathematical expression that describes the shape of an elastic lithosphere subject to loading at one end, expressed as:

$$\frac{w}{w_\mathrm{b}} = \sqrt{2}e^{\pi/4}\exp\left[-\frac{\pi}{4}\left(\frac{x-x_0}{x_\mathrm{b}-x_0}\right)\right]\sin\left[\frac{\pi}{4}\left(\frac{x-x_0}{x_\mathrm{b}-x_0}\right)\right] \quad (1)$$

where w is the deflection of the crust, w_b is the height of the forebulge, x_b is the position of the top of the forebulge, and x_0 is the position of the landward edge of the forebulge. When the origin point for x is set to x_0, $w/w_b = 0$ at $x = 0$ in Equation 1. The forebulge is postulated to be shallower than 6,300 m depth, which is the top of the oceanic crust in the abyssal plains far from the trench (Fujie et al., 2013). Therefore, x_0 is the point where the top of the oceanic crust is at 6,300 m depth at the trench slope. Then, w_b and x_b are derived by taking this derived position of x_0 as the origin and fitting Equation 1 to the observed top of the oceanic crust using the least squares method at the trench slope ($x < x_0$) for each survey line (Figure S7a in Supporting Information S1). We used only the subducted portion of the oceanic crust when calculating the RMS difference (Figure S7a in Supporting Information S1). By subtracting the depth of UFM from that of the top of the oceanic crust, we removed trend associated with subduction so that the shorter wavelength undulations could be evaluated (Figure 3b; the removal of the long wavelength component is shown in Table S2 in Supporting Information S1).

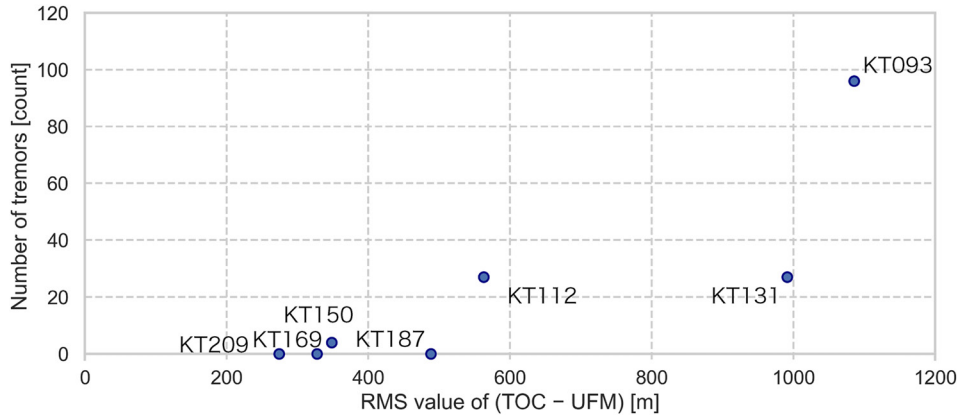

Figure 4. The relationship between the RMS difference between observed top of the subducted oceanic crust (TOC) and the expected (Universal Flexure Model) (see Table S2 in Supporting Information S1) and the number of shallow tremor occurrences along each survey line.

For survey lines in areas of active shallow tremors, RMS values ranged from 563 m to 1,085 m, averaging 880 m. In contrast, for lines in areas of few tremors (<10 counts), the RMS values ranged from 274 to 488 m, averaging 359 m. Comparison of the RMS values and tremor occurrences (Figure 4) confirms that regions of active shallow tremors tended to be near larger oceanic crust undulations. These findings are consistent with previous studies that have reported active tremors in areas with distinct structural variations, such as the northern Hikurangi Margin's subducted seamount (Todd et al., 2018) and the Hyuga-nada's subducted ridge (Yamashita et al., 2015, 2021). These features can lead to large RMS values compared to adjacent regions lacking such structures. Our findings could be supported by a modeling of fault slip behavior, which indicates that slow slip events are more likely to occur on faults with complex shapes (Tal et al., 2017).

In seismic reflection surveys, apparent depressions may result from the velocity structure. For example, detailed MCS surveys conducted in the Nankai Trough observed apparent arcuate depressions at the plate boundary that were attributed to a low-velocity zone detected in seismic refraction surveys (Nakamura et al., 2022). In our study area, however, previous refraction surveys have not observed any low velocity anomaly that might correspond to the observed undulations (Azuma et al., 2012; Nishizawa et al., 2009). Furthermore, our seismic data allow us to reliably determine velocities at shallow depths near the trench where undulations are observed. These observations suggest that the undulations are not apparent structures due to velocity structure variations, but true structures in the oceanic crust.

Shallow tremor occurrences correspond well to the scales of the amplitudes and wavelengths of the undulations in the oceanic crust and generally correspond to regions of strong plate-boundary reflections observed by Azuma et al. (2012) (Figure 1). They observed that interplate reflectivity varied from strong in the west to weak in the east, although the eastern edge of the strong reflections is at least 35 km farther east than the eastern limits of the shallow tremor distribution and the large-scale undulations. Nonetheless, this distance is shorter than the maximum wavelength (40 km) of the undulations. Therefore, we consider that the distributions of shallow tremors, large-scale undulations, and strong reflections are broadly consistent.

Strong reflections at plate boundaries may be due to the presence of fluid caused by undulations. The strength of seismic reflections is primarily attributed to differences in acoustic impedance, which is significantly influenced by the presence of fluid, with fluid inhomogeneities. Numerical models of a subducted seamount suggest that the seamount induce broad changes in tectonic overpressure (Ruh et al., 2016) and that pressurized fluid associated with the seamount is known to cause strong reflections in the Hikurangi subduction zone (Ellis et al., 2015). It is therefore possible that the undulations observed here cause strong reflections due to the presence of overpressured fluid.

It would be interesting to compare our results with an interseismic coupling model that suggests the possibility of locking over the entire plate boundary area off Hokkaido near the Kuril Trench (Itoh et al., 2021). However, they questioned the accuracy of the model near the trench due to a lack of seafloor geodetic data. Therefore, we do not

address a detailed comparison between our results and interseismic coupling models. This is a crucial issue that should be addressed in the future when seafloor geodetic data are available.

6. Conclusions

To investigate the origin of shallow tremor events in subduction zones, we performed a MCS reflection survey of the Kuril Trench off Hokkaido. We identified undulations in the subducted oceanic crust and quantitatively determined their amplitudes and wavelengths based on the deviation of the observed depth to the top of subducted oceanic crust from that expected from the UFM. We also determined the thickness of the frontal prism and the length of a strongly reflective zone in the oceanic crust. Each of these factors correlates with the shallow tremor distribution. Shallow tremors occur in areas with strong plate-boundary reflections, which are hypothesized to indicate fluid. Because large undulations in the oceanic crust should influence the hydrogeological variations of the plate boundary, the undulations may affect the occurrence of shallow tremors.

Data Availability Statement

The seismic data are available at JAMSTEC (2004), cruise IDs are KM20-E02 and KR19-07. Cruise reports for the surveys are available at Fujie (2019) and No (2020). Maps created using the Free and Open Source QGIS version 3.24 (QGIS.org., 2022).

Acknowledgments
The authors are grateful to the captains, crews, and marine technicians for their help during the seismic surveys. The authors thank Prof. Gaku Kimura for valuable comments and suggestions. We thank an editor, an associate editor and two anonymous reviewers, for their constructive reviews that helped improve the content of the manuscript. This work was supported by JST SPRING, Grant JPMJSP2148.

References

Argus, D. F., Gordon, R. G., & Mets, C. D. (2011). Geologically current motion of 56 plates relative to the no-net-rotation reference frame. *Geochemistry, Geophysics, Geosystems*, *12*(11). https://doi.org/10.1029/2011GC003751

Azuma, R., Murai, Y., Katsumata, K., Nishimura, Y., Yamada, T., Mochizuki, K., & Shinohara, M. (2012). Was the 1952 Tokachi-oki earthquake (Mw= 8.1) a typical underthrust earthquake?Plate interface reflectivity measurement by an air gun--ocean bottom seismometer experiment in the Kuril Trench. *Geochemistry, Geophysics, Geosystems*, *13*(8). https://doi.org/10.1029/2012GC004135

Barker, D. H., Henrys, S., Tontini, F. C., Barnes, P. M., Bassett, D., Todd, E., & Wallace, L. (2018). Geophysical constraints on the relationship between seamount subduction, slow slip, and tremor at the north Hikurangi subduction zone, New Zealand. *Geophysical Research Letters*, *45*(23). https://doi.org/10.1029/2018GL080259

Ellis, S., Fagereng, Å., Barker, D., Henrys, S., Saffer, D., Wallace, L., et al. (2015). Fluid budgets along the northern Hikurangi subduction margin, New Zealand: The effect of a subducting seamount on fluid pressure. *Geophysical Journal International*, *202*(1), 277–297. https://doi.org/10.1093/gji/ggv127

Fujie, G. (2019). R/V Kairei Cruise report KR19-07 [Dataset]. JAMSTEC. https://doi.org/10.17596/0002613

Fujie, G., Kodaira, S., Nakamura, Y., Morgan, J. P., Dannowski, A., Thorwart, M., et al. (2020). Spatial variations of incoming sediments at the northeastern Japan arc and their implications for megathrust earthquakes. *Geology*, *48*(6), 614–619. https://doi.org/10.1130/G46757.1

Fujie, G., Kodaira, S., Yamashita, M., Sato, T., Takahashi, T., & Takahashi, N. (2013). Systematic changes in the incoming plate structure at the Kuril trench. *Geophysical Research Letters*, *40*(1), 88–93. https://doi.org/10.1029/2012GL054340

GEBCO Compilation Group. (2022). GEBCO_2022 grid. https://doi.org/10.5285/e0f0bb80-ab44-2739-e053-6c86abc0289c

Hirata, K., Geist, E., Satake, K., Tanioka, Y., & Yamaki, S. (2003). Slip distribution of the 1952 Tokachi-Oki earthquake (M 8.1) along the Kuril Trench deduced from tsunami waveform inversion. *Journal of Geophysical Research*, *108*(B4). https://doi.org/10.1029/2002JB001976

Hua, Y., Zhao, D., Toyokuni, G., & Xu, Y. (2020). Tomography of the source zone of the great 2011 Tohoku earthquake. *Nature Communications*, *11*(1), 1163. https://doi.org/10.1038/s41467-020-14745-8

Itoh, Y., Nishimura, T., Wang, K., & He, J. (2021). New megathrust locking model for the southern Kurile subduction zone incorporating viscoelastic relaxation and non-uniform compliance of upper plate. *Journal of Geophysical Research: Solid Earth*, *126*(5). https://doi.org/10.1029/2020JB019981

JAMSTEC. (2004). JAMSTEC seismic survey database [Dataset]. Japan Agency for Marine-Earth Science and Technology. https://doi.org/10.17596/0002069

Kawakubo, S., Azuma, R., Hino, R., Takahashi, H., Ohta, K., & Shinohara, M. (2020). *Shallow low-frequency tremor activity off Erimo, Hokkaido from 2006 to 2007 revealed from pop-up type ocean bottom seismometers*. JpGU-AGU Joint Meeting. Retrieved from https://confit.atlas.jp/guide/event/jpgu2020/subject/SCG58-P29/detail?lang=en

KlaeschenDirk, B., GnibidenkoHelios, P., Gnibidenko, H., & von Huene, R. (1994). Structure of the Kuril Trench from seismic reflection records. *Journal of Geophysical Research*, *99*(B12), 24173–24188. https://doi.org/10.1029/94JB01186

Kodaira, S., Nakamura, Y., Yamamoto, Y., Obana, K., Fujie, G., No, T., et al. (2017). Depth-varying structural characters in the rupture zone of the 2011 Tohoku-oki earthquake. *Geosphere*, *13*(5), 1408–1424. https://doi.org/10.1130/GES01489.1

Mochizuki, K., Nakamura, M., Kasahara, J., Hino, R., Nishino, M., Kuwano, A., et al. (2005). Intense PP reflection beneath the aseismic forearc slope of the Japan Trench subduction zone and its implication of aseismic slip subduction. *Journal of Geophysical Research*, *110*(B1). https://doi.org/10.1029/2003JB002892

Nakamura, Y., Shiraishi, K., Fujie, G., Kodaira, S., Kimura, G., Kaiho, Y., et al. (2022). Structural anomaly at the boundary between strong and weak plate coupling in the central-western Nankai Trough. *Geophysical Research Letters*, *49*(10). https://doi.org/10.1029/2022GL098180

Nakanishi, A., Kurashimo, E., Tatsumi, Y., Yamaguchi, H., Miura, S., Kodaira, S., et al. (2009). Crustal evolution of the southwestern Kuril Arc, Hokkaido Japan, deduced from seismic velocity and geochemical structure. *Tectonophysics*, *472*(1–4), 105–123. https://doi.org/10.1016/j.tecto.2008.03.003

NIED. (2019). *NIED S-net*. National Research Institute for Earth Science and Disaster Resilience. https://doi.org/10.17598/nied.0007

Nishikawa, T., Ide, S., & Nishimura, T. (2023). A review on slow earthquakes in the Japan Trench. *Progress in Earth and Planetary Science*, *10*(1), 1. https://doi.org/10.1186/s40645-022-00528-w

Nishikawa, T., Matsuzawa, T., Ohta, K., Uchida, N., Nishimura, T., & Ide, S. (2019). The slow earthquake spectrum in the Japan Trench illuminated by the S-net seafloor observatories. *Science*, *365*(6455), 808–813. https://doi.org/10.1126/science.aax5618

Nishimura, T. (2009). Slip distribution of the 1973 Nemuro-oki earthquake estimated from the re-examined geodetic data. *Earth Planets and Space*, *61*(11), 1203–1214. https://doi.org/10.1186/BF03352973

Nishizawa, A., Kaneda, K., Watanabe, N., & Oikawa, M. (2009). Seismic structure of the subducting seamounts on the trench axis: Erimo Seamount and Daiichi-Kashima Seamount, northern and southern ends of the Japan Trench. *Earth Planet*, *61*(3), e5–e8. https://doi.org/10.1186/BF03352912

No, T. (2020). R/V KAIMEI cruise report KM20-E02 [Dataset]. JAMSTEC. https://doi.org/10.17596/0002556

Obana, K., & Kodaira, S. (2009). Low-frequency tremors associated with reverse faults in a shallow accretionary prism. *Earth and Planetary Science Letters*, *287*(1–2), 168–174. https://doi.org/10.1016/j.epsl.2009.08.005

Obara, K., & Kato, A. (2016). Connecting slow earthquakes to huge earthquakes. *Science*, *353*(6296), 253–257. https://doi.org/10.1126/science.aaf1512

Okamura, Y., Tsujino, T., Arai, K., Sasaki, T., Satake, K., & Joshima, M. (2008). Fore arc structure and plate boundary earthquake sources along the southwestern Kuril subduction zone. *Journal of Geophysical Research*, *113*(B6). https://doi.org/10.1029/2007JB005246

Park, J.-O., Hori, T., & Kaneda, Y. (2009). Seismotectonic implications of the Kyushu-Palau ridge subducting beneath the westernmost Nankai forearc. *Earth Planet*, *61*(8), 1013–1018. https://doi.org/10.1186/BF03352951

QGIS.org. (2022). QGIS 3.24. Geographic information system: February 18, 2022 release (version 3.24) [Software]. QGIS Association. Retrieved from http://www.qgis.org

Ruh, J. B., Sallarès, V., Ranero, C. R., & Gerya, T. (2016). Crustal deformation dynamics and stress evolution during seamount subduction: High-resolution 3-D numerical modeling. *JGR Solid Earth*, *121*(9), 6880–6902. https://doi.org/10.1002/2016JB013250

Schnürle, P., Lallemand, S. E., Huene, R. v., & Klaeschen, D. (1995). Tectonic regime of the southern Kuril Trench as revealed by multichannel seismic lines. *Tectnophysics*. https://doi.org/10.1016/0040-1951(94)00173-7

Sun, T., Saffer, D., & Ellis, S. (2020). Mechanical and hydrological effects of seamount subduction on megathrust stress and slip. *Nature Geoscience*, *13*(3), 249–255. https://doi.org/10.1038/s41561-020-0542-0

Tal, Y., Hager, B. H., & Ampuero, J. P. (2017). The effects of fault roughness on the earthquake nucleation process. *Journal of Geophysical Research: Solid Earth*, *123*(1), 437–456. https://doi.org/10.1002/2017JB014746

Tanioka, Y., Hirata, K., Hino, R., & Kanazawa, T. (2004). Slip distribution of the 2003 Tokachi-oki earthquake estimated from tsunami waveform inversion. *Earth Planets and Space*, *56*(3), 373–376. https://doi.org/10.1186/BF03353067

Todd, E. K., Schwartz, S. Y., Mochizuki, K., Wallace, L. M., Sheehan, A. F., Webb, S. C., et al. (2018). Earthquakes and tremor linked to seamount subduction during shallow slow slip at the Hikurangi margin, New Zealand. *Journal of Geophysical Research: Solid Earth*, *123*(8), 6769–6783. https://doi.org/10.1029/2018JB016136

Tsuru, T., Park, J. O., Kido, Y., Ito, A., Kaneda, Y., Yamada, T., et al. (2005). Did expanded porous patches guide rupture propagation in 2003 Tokachi-oki earthquake? *Geophysical Research Letters*, *32*(20). https://doi.org/10.1029/2005GL023753

Turcotte, D. L., & Schubert, G. (2001). Geodynamics (2nd ed.). https://doi.org/10.1017/CBO9780511807442

Tuzino, T., & Noda, A. (2010). Architecture and evolution of the Kushiro submarine canyon in the Kurile Trench forearc slope. North-western Pacific. https://doi.org/10.1111/j.1365-3091.2009.01107.x

von Huene, R., Ranero, C. R., & Scholl, D. W. (2009). *Convergent margin structure in high-quality geophysical images and current kinematic and dynamic models*. Springer. Subduction Zone Geodynamics. https://doi.org/10.1007/978-3-540-87974-9

Walter, J. I., Schwartz, S. Y., Protti, M., & Gonzalez, V. (2011). Persistent tremor within the northern Costa Rica seismogenic zone. *Geophysical Research Letters*, *38*(1). https://doi.org/10.1029/2010GL045586

Yamanaka, Y., & Kikuchi, M. (2003). Source process of the recurrent Tokachi-oki earthquake on September 26, 2003, inferred from teleseismic body waves. *Earth Planets and Space*, *55*(12), e21–e24. https://doi.org/10.1186/BF03352479

Yamashita, Y., Shinohara, M., & Yamada, T. (2021). Shallow tectonic tremor activities in Hyuga-nada, Nankai subduction zone, based on long-term broadband ocean bottom seismic observations. *Earth Planets and Space*, *73*(1), 196. https://doi.org/10.1186/s40623-021-01533-x

Yamashita, Y., Yakiwara, H., Asano, Y., Shimizu, H., Uchida, K., Hirano, S., et al. (2015). Migrating tremor off southern Kyushu as evidence for slow slip of a shallow subduction interface. *Science*, *348*(6235), 676–679. https://doi.org/10.1126/science.aaa4242

Yokota, Y., Ishikawa, T., Watanabe, S.-i., Tashiro, T., & Asada, A. (2016). Seafloor geodetic constraints on interplate coupling of the Nankai Trough megathrust zone. *Nature*, *534*(7607), 374–377. https://doi.org/10.1038/nature17632